Eur. Phys. J. A **11**, 209–216 (2001)

**THE EUROPEAN PHYSICAL JOURNAL A**



# Aspects of near-threshold neutral pion photoproduction off protons

V. Bernard[1,a], N. Kaiser[2,b], and U.-G. Meißner[3,c]

[1] Université Louis Pasteur, Laboratoire de Physique Théorique 3-5, rue de l'Université, F-67084 Strasbourg, France
[2] Technische Universität München, Physik Department T39 James-Franck-Straße, D-85747 Garching, Germany
[3] Forschungszentrum Jülich, Institut für Kernphysik (Theorie), D-52425 Jülich, Germany

Received: 25 May 2001 / Revised version: 20 June 2001
Communicated by A. Schäfer

**Abstract.** We investigate near-threshold neutral pion photoproduction off protons to fourth order in heavy-baryon chiral perturbation theory in the light of the new data from MAMI. We show that the unitarity cusp at the secondary $\pi^+ n$ threshold is in agreement with expectations from the final-state theorem. We also analyze the fourth-order corrections to the $P$-wave low-energy theorems and show that potentially large $\Delta$ isobar contributions are cancelled by sizeable pion loop effects. This solidifies the parameter-free third-order predictions, which are in good agreement with the data.

**PACS.** 12.20.Ds Specific calculations – 12.39.Fe Chiral Lagrangians – 25.20.Lj Photoproduction reactions

## 1 Introduction

Chiral perturbation theory is the tool to systematically investigate the consequences of the spontaneous and explicit chiral symmetry breaking in QCD. $S$-matrix elements and transition currents of quark operators are calculated with the help of an effective field theory formulated in terms of the asymptotically observed fields, the Goldstone bosons and the low-lying baryons. A systematic perturbative expansion in terms of small external momenta and meson masses is possible. We call this double expansion from here on *chiral expansion* and denote the small parameters collectively by $q$. Beyond leading order, coupling constants not fixed by chiral symmetry appear, the so-called low-energy constants (LECs). These have to be determined by a fit to some data or using some model. A large variety of processes such as pion-nucleon scattering, real and virtual Compton scattering and so on has already been investigated in this framework, sharpening our understanding of the chiral structure of QCD (for reviews, see, *e.g.* [1,2]).

Neutral pion photoproduction off protons and deuterons (which gives access to the elementary neutron amplitudes) is one of the prime processes to test our understanding of the chiral pion-nucleon dynamics for essentially two reasons. First, over the last decade fairly precise differential and total cross-section data have been obtained at MAMI [3–5] and SAL [6–8]. A further experiment involving linearly polarized photons was performed at MAMI, which not only improved the differential cross-sections but also gave the first determination of the photon asymmetry [9]. Second, the $S$-wave amplitude $E_{0+}$ is sensitive to a particular pion loop effect [10]. In the threshold region, the fourth-order heavy-baryon chiral perturbation theory calculation (HBCHPT) (which involves the sum $a_1 + a_2$ of two low-energy constants) agrees with what is found in the multipole analysis of the data [5, 11,12]. In addition, the rather counterintuitive prediction for the electric-dipole amplitude for $\pi^0$ photoproduction off the neutron, $|E_{0+}^{\pi^0 n}| > |E_{0+}^{\pi^0 p}|$ translates into a threshold deuteron amplitude $E_d$ [13] that was verified by a SAL experiment within 20% [8]. Moreover, in [11] it was also shown that there are two *$P$-wave low-energy theorems (LETs)* for the $P_{1,2}$ multipoles which show a rapid convergence based on the third-order calculation. While the LET for $P_1$ could be tested and verified from the unpolarized data, only the recent MAMI measurement of $\vec{\gamma} p \to \pi^0 p$ allows to disentangle the contribution from the $P_2$ and the $P_3$ multipoles (the latter being largely determined by the LEC $b_P$ at third order)[1]. It has been frequently argued that contributions from the delta isobar, that only appear at fourth order in the chiral expansion for $P_1$ and $P_2$, will not only spoil the rapid convergence of the $P$-wave LETs but also lead to numerically different values.

[a] e-mail: bernard@lpt6.u-strasbg.fr
[b] e-mail: nkaiser@physik.tu-muenchen.de
[c] e-mail: Ulf-G.Meissner@fz-juelich.de

[1] Note that the first but somewhat model-dependent comparison between $P$-wave multipoles and the LET predictions was given by Bergstrom [14].

This is witnessed, *e.g.*, in an effective field theory approach including the delta as an active degree of freedom [15] in which one counts the nucleon-delta mass splitting as another small parameter. A third-order analysis in that framework seems to indicate indeed large corrections rendering the agreement of the prediction for $P_1$ at threshold with the value deduced from the differential cross-sections as accidental [16].

In this paper, we complete the fourth-order (complete one loop) analysis based on HBCHPT by evaluating the corresponding corrections for the three $P$-wave multipoles. We use this framework to analyze the new data from MAMI, which confirms and sharpens previous findings concerning the electric-dipole amplitude $E_{0+}$ and sheds new light on the convergence issue of the $P$-wave LETs.

## 2 Formal aspects

In this section, we collect some basic formulas needed for describing the reaction $\gamma(k) + p(p_1) \to \pi^0(q) + p(p_2)$. In the threshold region, it is legitimate to consider $\pi^0$ photoproduction in $S$- and $P$-wave approximation, with the corresponding transition current matrix element given by

$$\frac{m}{4\pi\sqrt{s}} T \cdot \epsilon = i\vec{\sigma}\cdot\vec{\epsilon}\,[E_{0+}(\omega) + \hat{k}\cdot\hat{q}\,P_1(\omega)] + i\vec{\sigma}\cdot\hat{k}\,\vec{\epsilon}\cdot\hat{q}\,P_2(\omega) + (\hat{q}\times\hat{k})\cdot\vec{\epsilon}\,P_3(\omega)\,. \quad (1)$$

Here, $m = 938.27$ MeV is the proton mass, $s = (p_1+k)^2 = (p_2+q)^2$ the total centre-of-mass (cm) energy squared, $\omega = (s - m^2 + M_{\pi^0}^2)/2\sqrt{s}$ the cm energy of the produced neutral pion, and $\epsilon^\mu = (0, \vec{\epsilon})$ the polarization vector of the real photon in the Coulomb gauge subject to the transversality condition $\vec{\epsilon}\cdot\vec{k} = 0$. At threshold, the $\pi^0$ is produced at rest in the cm frame, $\vec{q} = 0$, so that $\omega_{\rm thr} = M_{\pi^0} = 134.97$ MeV corresponding to $\sqrt{s}_{\rm thr} = M_{\pi^0} + m$. The secondary $\pi^+ n$ threshold opens at $\omega_{\rm c} = 140.11$ MeV, where $\sqrt{s}_{\rm c} = M_{\pi^+} + m_n$ (with $m_n = 939.57$ MeV, the neutron mass). At that point, the strong unitary cusp related to the rescattering process $\gamma p \to \pi^+ n \to \pi^0 p$ occurs in the electric-dipole amplitude $E_{0+}(\omega)$. In the vicinity of the cusp its generic form reads $E_{0+}(\omega) = -a - b\sqrt{1-\omega^2/\omega_{\rm c}^2}$ with two constants $a$ and $b$. The amplitudes $P_{1,2,3}(\omega)$ are linear combinations of the more commonly used magnetic dipole ($M_{1\pm}$) and electric quadrupole ($E_{1+}$) $P$-wave pion photoproduction multipoles. The combinations $P_{1,2,3}(\omega)$ arise most naturally from the decomposition of the $T$-matrix in eq. (1). Of importance for the later discussion are also the threshold $P$-wave slopes $\overline{P}_{1,2}$, defined via

$$\overline{P}_{1,2} = \lim_{\vec{q}\to 0} \frac{P_{1,2}(\omega)}{|\vec{q}\,|}\,, \quad (2)$$

because for these, the LETs mentioned in the introduction have been derived in [11]. The differential cross-section and the photon asymmetry $\Sigma$ can be expressed in terms of the multipoles as

$$\frac{|\vec{k}\,|}{|\vec{q}\,|}\frac{{\rm d}\sigma}{{\rm d}\Omega_{\rm cm}} = A + B\,\cos\theta + C\,\cos^2\theta\,, \quad (3)$$

$$A = |E_{0+}|^2 + \frac{1}{2}|P_2|^2 + \frac{1}{2}|P_3|^2\,, \quad (4)$$

$$B = 2{\rm Re}(E_{0+}P_1^*)\,, \quad (5)$$

$$C = |P_1|^2 - \frac{1}{2}|P_2|^2 - \frac{1}{2}|P_3|^2\,, \quad (6)$$

$$\Sigma = \frac{|\vec{q}\,|\sin^2\theta}{2|\vec{k}\,|}\left(\frac{{\rm d}\sigma}{{\rm d}\Omega_{\rm cm}}\right)^{-1}\left(|P_3|^2 - |P_2|^2\right), \quad (7)$$

with $\theta$, the cm scattering angle and we have dropped the argument $\omega$.

## 3 Chiral expansion of the multipoles

We wish to calculate the $T$-matrix element, eq. (1), to order $\mathcal{O}(q^4)$. For the electric-dipole amplitude $E_{0+}(\omega)$, this has been already done in [11]. In that paper, also the third-order terms for the $P$-wave multipoles $P_{1,2,3}(\omega)$ were evaluated. Here, we give these up to and including fourth order. We make use of the standard heavy-baryon effective chiral Lagrangian, which has been given to complete one loop accuracy, *i.e.* $\mathcal{O}(q^4)$, in ref. [17]. The expressions for the multipoles split in three parts. First, one has the (renormalized) Born terms which subsume the lowest-order couplings ($g_{\pi N}, m$) complemented by the anomalous magnetic moment ($\kappa_p$) contributions together with all pion loop corrections of these parameters at order $\mathcal{O}(q^3)$ and $\mathcal{O}(q^4)$. Secondly, there are the pion loop graphs with at most one insertion from the dimension two Lagrangian $\mathcal{L}_{\pi N}^{(2)}$. For these, the one-nucleon reducible parts which just renormalize the Born terms are taken out. Thirdly, there are the one-nucleon irreducible counterterm contributions which lead to simple polynomial amplitudes.

Consider first the renormalized Born terms which are expressed in terms of the physical parameters $g_{\pi N}, m, \kappa_p$. The second- and third-order terms for $P_{1,2,3}^{\rm Born}(\omega)$ are given in the appendix of ref. [11]. We display here only the novel fourth-order contributions

$$P_1^{\rm Born}(\omega) = \frac{e g_{\pi N}\,|\vec{q}\,|}{320\pi m^4} \times\left\{\frac{4M_\pi^4}{\omega^2} + (21+19\kappa_p)M_\pi^2 + (20+6\kappa_p)\omega^2\right\}, \quad (8)$$

$$P_2^{\rm Born}(\omega) = \frac{e g_{\pi N}\,|\vec{q}\,|}{320\pi m^4} \times\left\{\frac{4M_\pi^4}{\omega^2} - (43+15\kappa_p)M_\pi^2 - (26+10\kappa_p)\omega^2\right\}, \quad (9)$$

$$P_3^{\rm Born}(\omega) = \frac{e g_{\pi N}\,|\vec{q}\,|}{160\pi m^4}\left\{(3\kappa_p - 2)M_\pi^2 - (13+8\kappa_p)\omega^2\right\}, \quad (10)$$

with $|\vec{q}\,| = \sqrt{\omega^2 - M_\pi^2}$. From now on, $M_\pi = 134.97$ MeV denotes the neutral pion mass, $g_{\pi N} = 13.1$ is the strong pion-nucleon coupling constant and $\kappa_p = 1.793$ the anomalous magnetic moment of the proton.

Next, we give the $P$-wave contributions from the fourth-order one loop graphs. According to their prefactor, $g_A$ or $g_A^3$, these fall into two classes. In these loop

diagrams charged as well as neutral pions occur in internal lines and we have neglected throughout the small mass difference $M_{\pi^+} - M_{\pi^0} = 4.6$ MeV. In sharp contrast to the $S$-wave amplitude $E_{0+}$ (having a strong cusp effect) this approximation is legitimate for $P$-wave amplitudes since their imaginary parts and consequently their cusp effects are extremely tiny corrections. The numerical differences which result from taking the charged or neutral pion mass for $M_\pi$ should be regarded as an intrinsic inaccuracy of our $\mathcal{O}(q^4)$ calculation.

First, we give the analytical expressions for the $\mathcal{O}(q^4)$ loops proportional to $g_A$:

$$P_1^{\rm loop}(\omega) = \frac{eg_A\,|\vec{q}\,|}{m(4\pi F_\pi)^3}\bigg\{\Big(3+\frac{8}{3}\tilde{c}_4\Big)\omega^2\ln\frac{M_\pi}{\lambda} + \frac{4}{9}\tilde{c}_4(6M_\pi^2-5\omega^2) + \frac{M_\pi^2}{2}\arcsin^2\frac{\omega}{M_\pi} - \frac{8\tilde{c}_4}{3\omega}(M_\pi^2-\omega^2)^{3/2}\arcsin\frac{\omega}{M_\pi} + \omega\sqrt{M_\pi^2-\omega^2} \times \arcsin\frac{\omega}{M_\pi} + \frac{2\omega^3}{\sqrt{M_\pi^2-\omega^2}}\arccos\frac{\omega}{M_\pi}\bigg\}, \quad (11)$$

$$P_2^{\rm loop}(\omega) = \frac{eg_A\,|\vec{q}\,|}{m(4\pi F_\pi)^3}\bigg\{-\Big(2+\frac{4}{3}\tilde{c}_4\Big)\omega^2\ln\frac{M_\pi}{\lambda} + \omega^2 + \frac{8}{9}\tilde{c}_4(3M_\pi^2+2\omega^2) - 2\tilde{c}_4M_\pi^2\arcsin^2\frac{\omega}{M_\pi} + \frac{\pi}{2}\Big[\omega\sqrt{M_\pi^2-\omega^2} - M_\pi^2\arcsin\frac{\omega}{M_\pi}\Big] - \Big[2\omega+\frac{4\tilde{c}_4}{3\omega}(\omega^2+2M_\pi^2)\Big]\sqrt{M_\pi^2-\omega^2}\arcsin\frac{\omega}{M_\pi}\bigg\}, \quad (12)$$

$$P_3^{\rm loop}(\omega) = \frac{eg_A\,|\vec{q}\,|}{m(4\pi F_\pi)^3} \times\bigg\{-\frac{\pi}{2}(1+4\tilde{c}_4)\Big[\omega\sqrt{M_\pi^2-\omega^2}+M_\pi^2\arcsin\frac{\omega}{M_\pi}\Big]\bigg\}, \quad (13)$$

with $F_\pi = 92.4$ MeV, the weak pion decay constant; $\kappa_n = -1.913$, the neutron magnetic moment; $g_A = g_{\pi N}F_\pi/m = 1.29$ and $\tilde{c}_4 = mc_4$. The low-energy constant $c_4$ has been determined from pion-nucleon scattering inside the Mandelstam triangle as $c_4 = 3.4$ GeV$^{-1}$ [18]. $\lambda$ is the scale of dimensional regularization which will be set equal to $\lambda = m$. As a check, these loop contributions fulfill the condition $P_{1,2,3}^{\rm loop}(0) = 0$ which confirms that all one-nucleon reducible pieces are indeed taken out. The analytical continuation above threshold $\omega > M_\pi$ is obtained by the following substitutions:

$$\sqrt{M_\pi^2-\omega^2} \to -i\,\sqrt{\omega^2-M_\pi^2}\,, \qquad \arcsin\frac{\omega}{M_\pi} \to \frac{\pi}{2} + i\,\ln\frac{\omega+\sqrt{\omega^2-M_\pi^2}}{M_\pi}\,. \quad (14)$$

Similar analytical expressions are found for the other class of $\mathcal{O}(q^4)$ loops proportional to $g_A^3$,

$$P_1^{\rm loop}(\omega) = \frac{eg_A^3\,|\vec{q}\,|}{m(4\pi F_\pi)^3}\bigg\{\frac{\omega^2}{3}(7+4\kappa_p+2\kappa_n)\ln\frac{M_\pi}{\lambda} - \frac{(M_\pi^2-\omega^2)^{3/2}}{3\omega}(7+4\kappa_p+2\kappa_n)\arcsin\frac{\omega}{M_\pi} + \frac{\pi M_\pi^2}{6\omega^3} \times\bigg[4M_\pi^3 - 6\omega^2M_\pi - \frac{3\omega^4}{M_\pi} + 3\omega(2\omega^2-M_\pi^2)\arcsin\frac{\omega}{M_\pi} + (7\omega^2-4M_\pi^2)\sqrt{M_\pi^2-\omega^2}\bigg] + \frac{M_\pi^2}{6}(17+8\kappa_p+4\kappa_n) - \frac{\omega^2}{9} \times(19+10\kappa_p+5\kappa_n) + \frac{M_\pi^2}{2\omega^2}(\omega^2-M_\pi^2)\arcsin^2\frac{\omega}{M_\pi}\bigg\}, \quad (15)$$

$$P_2^{\rm loop}(\omega) = \frac{eg_A^3\,|\vec{q}\,|}{m(4\pi F_\pi)^3}\bigg\{-\frac{2}{3}(5+2\kappa_p+\kappa_n)\omega^2\ln\frac{M_\pi}{\lambda} + \frac{\omega^2}{9}(19+10\kappa_p+5\kappa_n) + \frac{\sqrt{M_\pi^2-\omega^2}}{3\omega}\Big[M_\pi^2(7+4\kappa_p+2\kappa_n) - 2\omega^2(5+2\kappa_p+\kappa_n)\Big]\arcsin\frac{\omega}{M_\pi} - \frac{M_\pi^4}{2\omega^2}\arcsin^2\frac{\omega}{M_\pi} + \frac{\pi M_\pi}{6\omega^3}\Big[4M_\pi^4 - 6\omega^2M_\pi^2 + 3\omega^4 - 4M_\pi(M_\pi^2-\omega^2)^{3/2}\Big] - \frac{M_\pi^2}{6}(11+8\kappa_p+4\kappa_n)\bigg\}, \quad (16)$$

$$P_3^{\rm loop}(\omega) = \frac{eg_A^3\,|\vec{q}\,|}{m(4\pi F_\pi)^3} \times\bigg\{\frac{\pi}{3\omega}(\kappa_n-3\kappa_p-3)\Big[M_\pi^3-(M_\pi^2-\omega^2)^{3/2}\Big]\bigg\}, \quad (17)$$

which also fulfill the nontrivial condition $P_{1,2,3}^{\rm loop}(0) = 0$.

Finally, we are left with the polynomial counterterm contributions:

$$P_1^{\rm ct}(\omega) = \frac{eg_A\,|\vec{q}\,|\,\omega^2}{m(4\pi F_\pi)^3}\,\xi_1(\lambda)\,, \quad (18)$$

$$P_2^{\rm ct}(\omega) = \frac{eg_A\,|\vec{q}\,|\,\omega^2}{m(4\pi F_\pi)^3}\,\xi_2(\lambda)\,, \quad (19)$$

$$P_3^{\rm ct}(\omega) = e\,|\vec{q}\,|\,b_P\Big\{\omega - \frac{M_\pi^2}{2m}\Big\}\,. \quad (20)$$

The introduced new parameters (LECs) $\xi_{1,2}(\lambda)$ are dimensionless and they balance of course the scale dependence appearing in the fourth-order loop contribution via the chiral logarithm $\ln(M_\pi/\lambda)$. The form of $P_3^{\rm ct}(\omega)$ follows from the relativistic operators $O_8$ and $O_9$ constructed in ref. [17]. The LEC $b_P$ already appeared at third order, the only new feature here is a kinematical correction $|\vec{k}\,| = \omega - M_\pi^2/2m + \ldots$, which at threshold amounts to a 7% reduction.

Furthermore, we give the resonance contributions to the low-energy constants $\xi_{1,2}$ and $b_P$. As mentioned in ref. [11] there is a small contribution to $b_P$ from $t$-channel vector meson exchange ($\rho^0(770)$ and $\omega(782)$) and consequently also an analogous vector meson exchange contribution to $\xi_{1,2}$,

$$b_P^{(\rm V)} = \frac{5}{(4\pi F_\pi)^3}\,, \qquad \xi_1^{(\rm V)} = -2\xi_2^{(\rm V)} = -\frac{8}{g_A}\,. \quad (21)$$

Here, we have used various simplifying relations (see ref. [11]) for the vector meson coupling constants together

with the KSFR relation for the vector meson masses $M_\rho \simeq M_\omega$. The dominant contribution to $b_P$ and $\xi_{1,2}$ come from the low-lying $\Delta(1232)$ resonance. In refs. [11,12] we used a relativistic tree level approach in which the delta contribution is parametrized in terms of four couplings $g_1$, $g_2$, $Y$ and $Z$. The latter two are so-called off-shell parameters emerging in a relativistic description of the spin-3/2 fields. In a corresponding effective Lagrangian, these would be represented by some higher-order contact interactions. In fact, most of the delta resonance physics can be represented by the static isobar approach, which can be thought of as the leading term in a systematic effective field theory expansion like the one given in [15]. In the study of pion-nucleon scattering [19] it was already demonstrated that the dominant isobar contributions come indeed from the lowest-order Born graphs. Therefore, we use here the static nonrelativistic isobar model where one gets the following expressions:

$$b_P^{(\Delta)} = \frac{\kappa^*\, g_A}{6\sqrt{2}\pi m F_\pi}\, \frac{\Delta}{\Delta^2 - M_\pi^2}\,, \tag{22}$$

$$\xi_1^{(\Delta)} = -\xi_2^{(\Delta)} = \frac{\kappa^*}{3\sqrt{2}}\, \frac{(4\pi F_\pi)^2}{\Delta^2 - M_\pi^2}\,, \tag{23}$$

with $\Delta = 293$ MeV, the delta-nucleon mass splitting and $\kappa^*$ the $N\Delta$ transition magnetic moment. It is important for the numerical evaluation to keep the $M_\pi^2$-term in the denominator, this is also justified in the small scale expansion, where one counts $\Delta$ as a small parameter like the pion mass.

For the later discussion of the $P$-wave LETs, we now give the various contributions to the slopes $\overline{P}_{1,2}$. We start with the renormalized Born terms expressed by the physical pion-nucleon coupling constant $g_{\pi N}$, the renormalized anomalous magnetic moment $\kappa_p$ and the proton mass $m$. Furthermore, we introduce the small parameter $\mu = M_{\pi^0}/m \simeq 0.144$ and have

$$\overline{P}_1(\mathrm{Born}) = \frac{e g_{\pi N}}{8\pi m^2}\left[1 + \kappa_p - \frac{\mu}{2}(2+\kappa_p) + \frac{\mu^2}{8}(9+5\kappa_p)\right], \tag{24}$$

$$\overline{P}_2(\mathrm{Born}) = \frac{e g_{\pi N}}{8\pi m^2}\left[-1 - \kappa_p + \frac{\mu}{2}(3+\kappa_p) - \frac{\mu^2}{8}(13+5\kappa_p)\right]. \tag{25}$$

Here, novel terms of order $\mu^2$ appear. The result for the chiral loops at order $\mathcal{O}(q^3)$ can be taken from [11]:

$$\overline{P}_1(q^3 - \mathrm{loop}) = \frac{e g_{\pi N}^3\, \mu}{384\pi^2 m^2}(10 - 3\pi)\,, \tag{26}$$

$$\overline{P}_2(q^3\text{–loop}) = -\frac{e g_{\pi N}^3 \mu}{192\pi^2 m^2}\,. \tag{27}$$

These contributions are known to be quite small. From the formulae for $P_{1,2}^{\mathrm{loop}}(\omega)$ and $P_{1,2}^{\mathrm{ct}}(\omega)$ given above, one can readily deduce the terms due to the chiral loops and counterterms at order $\mathcal{O}(q^4)$:

$$\overline{P}_1(q^4\text{–loop, ct}) = \frac{e g_A M_\pi^2}{m(4\pi F_\pi)^3}\left\{\left[\frac{8}{3}\tilde{c}_4 + 3 + \frac{g_A^2}{3}(7 + 4\kappa_p + 2\kappa_n)\right]\ln\frac{M_\pi}{\lambda} - g_A^2\frac{5\pi}{6} + (1+2g_A^2)\frac{\pi^2}{8} + \frac{4}{9}\tilde{c}_4 + 2 + \frac{g_A^2}{18}(13 + 4\kappa_p + 2\kappa_n) + \xi_1(\lambda)\right\}, \tag{28}$$

$$\overline{P}_2(q^4\text{–loop, ct}) = \frac{e g_A M_\pi^2}{m(4\pi F_\pi)^3}\left\{\left[-\frac{4}{3}\tilde{c}_4 - 2 - \frac{2g_A^2}{3}(5 + 2\kappa_p + \kappa_n)\right]\ln\frac{M_\pi}{\lambda} + g_A^2\frac{\pi}{6} - (4\tilde{c}_4 + 2 + g_A^2)\frac{\pi^2}{8} + \frac{40}{9}\tilde{c}_4 + 1 + \frac{g_A^2}{18}(5 - 4\kappa_p - 2\kappa_n) + \xi_2(\lambda)\right\}. \tag{29}$$

The resulting numerical values will be given later.

## 4 Results and discussion

The new MAMI differential cross-section data span the energy range from $E_\gamma = 145.1$ MeV to 165.6 MeV in steps of about 1.1 MeV. In addition, the photon asymmetry $\Sigma$ has been evaluated for energies from 145 to 166 MeV, all these data for $\Sigma$ have been binned to one average energy of $E_\gamma = 159.5$ MeV. In total, we have 171 differential cross-section data, 19 total cross-section points and 7 data points for the photon asymmetry $\Sigma$.

First, it is instructive to compare the new data with the previously obtained ones of Fuchs *et al.* [4]. For doing that, we compare fits using the fourth-order expressions for the $S$-wave amplitude $E_{0+}$ and the third-order ones for the $P$-wave amplitudes (as it was done in [11,12]). The resulting LECs and $\chi^2$/dof are collected in table 1.

In both cases the two $S$-wave LECs are completely anticorrelated, *i.e.* only the sum $a_1 + a_2$ is of relevance. It agrees within 10% for the two fits, showing that the $S$-wave multipole $E_{0+}$ is internally consistent. The $P$-wave LEC $b_P$ is somewhat increased, but now consistent with the value obtained from fitting the SAL data [6,7], $b_P^{\mathrm{SAL}} \simeq 15\,\mathrm{GeV}^{-3}$ [12]. This can simply be traced back to the fact that the new MAMI total cross- sections are larger than the old ones above the secondary $\pi^+ n$ threshold. It is gratifying that this so far puzzling experimental discrepancy is now resolved.

Next, we wish to investigate the strength of the $S$-wave cusp. For that, we use the realistic two-parameter model developed in ref. [11] (which is similar to the so-called unitary fit of ref. [5]), where $E_{0+}$ is given by

$$E_{0+}(\omega) = -a - b\sqrt{1 - \frac{\omega^2}{\omega_{\mathrm{c}}^2}}\,. \tag{30}$$

Assuming isospin invariance for $\pi N$ rescattering, the strength of the cusp given by the parameter $b$ =

**Table 1.** Values of the LECs resulting from a three-parameter fit to the cross-section data of ref. [4] and [9]. Corr denotes correlation between the two $S$-wave LECs.

| | Schmidt *et al.* | Fuchs *et al.* |
|---|---|---|
| $a_1$ [GeV$^{-4}$] | 10.585 | 3.464 |
| $a_2$ [GeV$^{-4}$] | −4.542 | 3.136 |
| Corr$(a_1, a_2)$ | −0.998 | −0.999 |
| $a_1 + a_2$ [GeV$^{-4}$] | 6.04 | 6.60 |
| $b_P$ [GeV$^{-3}$] | 14.84 | 13.00 |
| No. of data | 190 | 180 |
| $\chi^2$/dof | 3.19 | 2.20 |

$\sqrt{2}\, a^- \, M_\pi \, E_{0+}^{\pi^+ n}$ can be inferred from the well-measured pion-nucleon scattering length $a(\pi^- p \to \pi^0 n)$ and the precise CHPT prediction for the electric-dipole amplitude $E_{0+}(\gamma p \to \pi^+ n)$ at threshold (which agrees with the data). This gives $b = (3.67 \pm 0.14) \cdot 10^{-3}/M_{\pi^+}$ [5]. Fitting the older MAMI data, the resulting value for $b$ came out sizeably smaller, $b \simeq 2.8 \cdot 10^{-3}/M_{\pi^+}$ [12]. This prompted some speculations that the strength of the unitary cusp is very sensitive to isospin violation. If, however, we use this same model together with the third-order predictions for the $P$-waves and apply it to the new MAMI data, we get

$$\begin{aligned} a &= 0.54 \cdot 10^{-3}/M_{\pi^+}\,, \\ b &= 3.63 \cdot 10^{-3}/M_{\pi^+}\,, \\ b_P &= 14.43 \text{ GeV}^{-3}\,, \end{aligned} \tag{31}$$

with a $\chi^2$/dof of 3.21, which is of the same quality as the one of the three parameter HBCHPT fit discussed before. The value for $b$ in eq. (31) is in perfect agreement with the prediction obtained from the final-state theorem and assuming isospin invariance for $\pi N$ rescattering. That sheds some doubt on the speculation that a precise measurement of the unitary cusp would be a good tool to investigate isospin violation. The resulting real part of $E_{0+}$ is given by the dash-dotted line in fig. 1.

In this simple three-parameter approach, one can also predict the photon asymmetry $\Sigma$, since $P_3$ is governed by the LEC $b_P$ and $P_2$ is given by the LET. Of course, in the full fit involving also the fourth-order contribution to the $P$-waves, one has additional terms from loops and counterterms, nevertheless, in this simplified ansatz one can already estimate the corrections to be expected from these additional terms. Using the LECs collected in table 1, we obtain the dash-dotted line in fig. 2, which agrees quite well with the data from the MAMI analysis. Therefore, we conclude that the corrections to the $P_2$ multipole should be small. Also, we had already noted before that $P_3$ is only modified on the percent level by the fourth-order corrections. Thus, to keep the fine balance between $|P_2|^2$ and $|P_3|^2$, which governs the size of $\Sigma$, only modest corrections to $P_2$ should be expected.

We now discuss the full fits including the fourth-order corrections to the $P$-wave multipoles $P_{1,2,3}(\omega)$. We have performed two types of fits. In set I, we only fit to the differential and total cross-section data excluding the photon asymmetry $\Sigma$. For set II, we include the photon asymmetry data in the fits. Let us first discuss the electric-dipole amplitude. It should come out to be (largely) independent of the fitting procedure since $\Sigma$ is only indirectly sensitive to the $S$-wave. The resulting LECs are collected in table 2. As expected, one finds a very similar result for $a_1 + a_2$ in agreement with the previous determinations. The resulting $E_{0+}(\omega)$ comes out indeed to be independent of the fitting procedure, as shown by the solid and dashed lines in fig. 1. It is in good agreement with determinations based on the older MAMI and the SAL data, which lead to $E_{0+}(\omega_{\rm thr}) = -(1.3 \pm 0.2) \cdot 10^{-3}/M_{\pi^+}$ and also with the result obtained from the new MAMI data, $E_{0+}(\omega_{\rm thr}) = -(1.33 \pm 0.08 \pm 0.03) \cdot 10^{-3}/M_{\pi^+}$. Therefore, even though the convergence of the chiral expansion

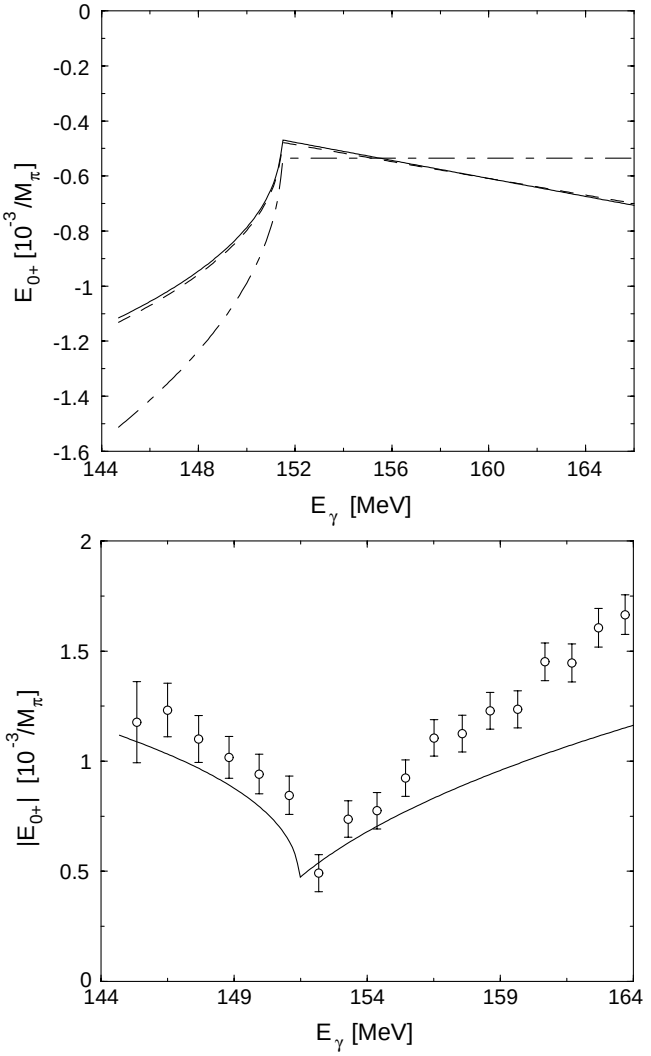


**Fig. 1.** The electric-dipole amplitude in the threshold region. Upper panel: real part. Dash-dotted line: two-parameter model for the electric dipole amplitude. Solid/dashed line: full CHPT fits corresponding to sets I/II of the parameters. Lower panel: the modulus of $E_{0+}$ for the full fit (see text) in comparison to the SAL data [6,7].

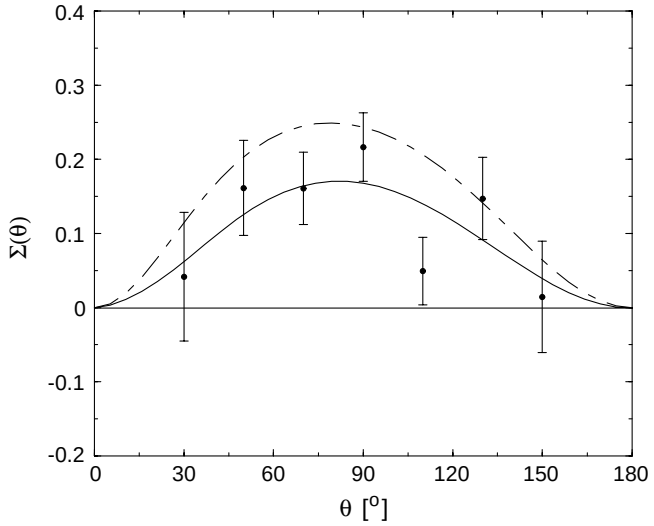


**Fig. 2.** The photon asymmetry at $E_\gamma = 159.5$ MeV. Dash-dotted line: prediction of the two-parameter model for the electric dipole amplitude. Solid line: full CHPT fit including the photon asymmetry data (set II). The data are from [9].

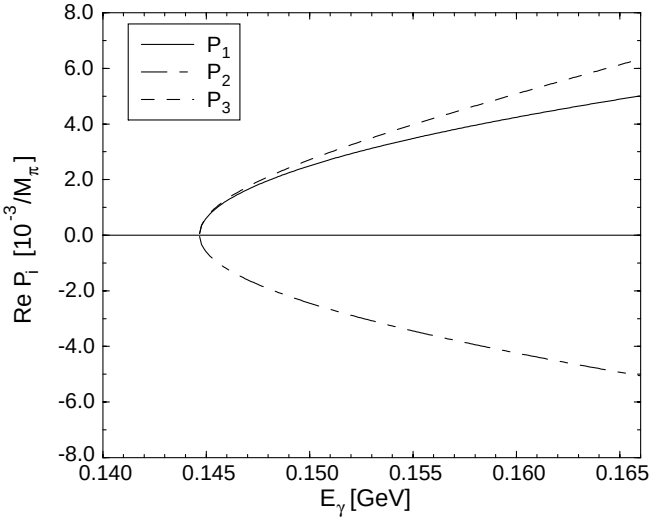


**Fig. 3.** Real part of the $P$-waves $P_i$ $(i = 1, 2, 3)$ *versus* photon energy.

**Table 2.** Values of the $S$-wave LECs and $E_{0+}$ at the two thresholds resulting from the five-parameter fits of the data of ref. [9]. Corr$(a_1, a_2)$ denotes correlation between the two $S$-wave LECs.

| | Set I | Set II |
|---|---|---|
| $a_1$ [GeV$^{-4}$] | 7.734 | 8.588 |
| $a_2$ [GeV$^{-4}$] | −1.506 | −2.288 |
| Corr$(a_1, a_2)$ | −0.998 | −0.998 |
| $a_1 + a_2$ [GeV$^{-4}$] | 6.23 | 6.30 |
| $\chi^2$/dof | 1.36 | 1.35 |
| $E_{0+}(\omega_{\rm thr})$ $[10^{-3}/M_{\pi+}]$ | −1.13 | −1.12 |
| $E_{0+}(\omega_{\rm c})$ $[10^{-3}/M_{\pi+}]$ | −0.53 | −0.52 |

in this multipole is slow, the fourth-order calculation is able to describe it in the threshold region with one parameter (the sum of LECs $a_1 + a_2$). This small value for $E_{0+}$ at threshold clearly establishes the large pion loop effect first pointed out in [10]. For completeness, we also show in fig. 1 the modulus of the electric-dipole amplitude, $|E_{0+}| = ([\mathrm{Re}\ E_{0+}]^2 + [\mathrm{Im}\ E_{0+}]^2)^{1/2}$, in comparison to the data from SAL [6,7], which nicely shows the unitary cusp.

We now turn to the $P$-waves. Here, we encounter the following problem. While the best fit of type I gives a good $\chi^2$/dof, see table 2, there is an almost perfect correlation between $b_P$, $\xi_1$ and $\xi_2$ (which is expected since the differential cross-sections are only sensitive to $|P_2|^2 + |P_3|^2$) and the resulting values for $b_P$ or $\xi_2$ come out either too large (based on expectations from resonance exchange, to be discussed below) or with too large uncertainty. We have also performed fits with fixing $b_P$ at the previously determined value of 14.8 GeV$^{-3}$, which gives almost the same $\chi^2$/dof but a wastly different value for $\xi_2$. Furthermore, including the leading effects of $D$-waves in the low-energy region does not change this. On the other hand, in all cases the LEC $\xi_1$ comes out in a narrow range, which is in agreement with the estimates based on resonance exchange to be discussed next. If one includes the photon asymmetry data, the cross-sections and the photon asymmetry are well described, see the solid line in fig. 2, but the resulting value for $b_P$ is too large, whereas $\xi_1$ and $\xi_2$ come out of the size expected from resonance saturation. For completeness, we show the energy dependence of the real parts of the $P$-wave multipoles for the fit including the asymmetry data in fig. 3.

Therefore, to get a more reliable estimate of the corrections to the $P$-wave LETs, we employ the resonance saturation hypothesis. First, taking the parameters used here, the LET predictions read (which are nothing but the sum of the third-order renormalized Born and loop terms):

$$\overline{P}_1^{\rm LET} = \quad 0.469\ \mathrm{GeV}^{-2}, \qquad [0.445, 0.492]\ \mathrm{GeV}^{-2},$$
$$\overline{P}_2^{\rm LET} = -0.498\ \mathrm{GeV}^{-2}, \quad [-0.472, -0.523]\ \mathrm{GeV}^{-2}, \quad (32)$$

where the numbers in the square brackets refer to a 5% theoretical uncertainty. The results based on the new MAMI data are [9]:

$$\overline{P}_1^{\rm exp} = \quad (0.441 \pm 0.004 \pm 0.013)\ \mathrm{GeV}^{-2},$$
$$\overline{P}_2^{\rm exp} = (-0.440 \pm 0.005 \pm 0.013)\ \mathrm{GeV}^{-2}, \quad (33)$$

which are in good agreement with the LET predictions. From our fourth-order results, we get for the sum of renormalized Born, third- and fourth-order loop and counterterm contributions

$$\overline{P}_1 = \quad (0.460 + 0.017 - 0.133 + 0.0048\,\xi_1)\ \mathrm{GeV}^{-2}\,, \quad (34)$$
$$\overline{P}_2 = -(0.449 + 0.058 - 0.109 + 0.0048\,\xi_2)\ \mathrm{GeV}^{-2}\,, \quad (35)$$

where the $\xi_{1,2}$ only depend on the $N\Delta$ transition magnetic moment. We note the rather sizeable (25%) correction from the fourth-order loops which at first sight seems

**Table 3.** Prediction for the $P$-wave slopes for variations of the $N\Delta$ transition magnetic moment $\kappa^*$.

| $\kappa^*$ | $\overline{P}_1$ [GeV$^{-2}$] | $\overline{P}_2$ [GeV$^{-2}$] |
|---|---|---|
| 4.0 | 0.408 | −0.475 |
| 4.5 | 0.416 | −0.487 |
| 5.0 | 0.427 | −0.498 |
| 5.5 | 0.439 | −0.509 |
| 6.0 | 0.450 | −0.521 |
| 6.5 | 0.461 | −0.532 |

to destroy the agreement between the LETs and the data. However, it is known that $\kappa^* \simeq 4\ldots6$, so we collect in table 3 the predictions for $\overline{P}_{1,2}$ for reasonable variations of $\kappa^*$. We see that for $\kappa^* = 4$, the delta contribution almost completely cancels the large fourth-order loop effect and thus the predictions for the $P$-wave slopes are within 7% of the empirical values. Note, however, that the empirical finding $\overline{P}_1^{\rm exp} = -\overline{P}_2^{\rm exp}$ is difficult to reconcile with any theory. For easier comparison with other calculations, one can express the dependence of $\Gamma(\Delta \to N\gamma)$ on the transition magnetic moment $\kappa^*$ in terms of the helicity amplitudes $A_{1/2}$ and $A_{3/2}$

$$\Gamma(\Delta^+ \to p\gamma) = \frac{k_\gamma^2 m}{2\pi m_\Delta}\Big(|A_{1/2}|^2 + |A_{3/2}|^2\Big)\,,$$
$$k_\gamma = \frac{m_\Delta^2 - m^2}{2m_\Delta}\,, \qquad (36)$$

to be compared with the formula obtained in a fully relativistic calculation (for details see appendix E in ref. [1]):

$$\Gamma(\Delta^+ \to p\gamma) = \frac{e^2\kappa^{*2}}{72\pi m_\Delta^2 m^2}(3m_\Delta^2 + m^2)k_\gamma^3$$
$$\simeq \kappa^{*2}\, 28.55 \text{ keV}\,. \qquad (37)$$

Using now the empirical values $A_{1/2} = (-0.135 \pm 0.006)\,\text{GeV}^{-1/2}$ and $A_{3/2} = (-0.255 \pm 0.008)\,\text{GeV}^{-1/2}$ [20] leads to $\kappa^* = 4.86$ with a much smaller uncertainty than given in table 3. However, we still give this somewhat larger range for $\kappa^*$ to better display the sensitivity of our results to this parameter.

## 5 Summary

In this paper, we have studied near-threshold neutral pion photoproduction off protons in the framework of heavy-baryon chiral perturbation theory to complete one loop (fourth-order) accuracy, updating and extending previous works on this topic [11,12]. The pertinent results of this investigation can be summarized as follows:

i) We have given the fourth-order corrections (loops and counterterms) to the three $P$-wave multipoles $P_{1,2,3}$. Two new low-energy constants appear, one for $P_1$ and the other for $P_2$. We have also given analytic expressions for the corrections to the low-energy theorems for the $P$-wave slopes $\overline{P}_{1,2}$, see eqs. (28),(29).

ii) We have analyzed the new MAMI data [9] first in the same approximation as it was done in previous works (*i.e.* the $P$-waves to third-order only). Using a realistic two-parameter model for the energy dependence of the electric-dipole amplitude $E_{0+}$, we have extracted the strength of the unitary cusp which agrees with the prediction based on the final-state theorem.

iii) Using the full one loop amplitude, one can fit the cross-section data and the photon asymmetry. The combination of $S$-wave LECs is stable and agrees with previous determinations, leading to $E_{0+}(\omega_{\rm thr}) = -1.1 \cdot 10^{-3}/M_{\pi^+}$. Two of the three $P$-wave LECs are not well determined because of strong correlations. More photon asymmetry data are needed to cure this situation.

iv) We have analyzed the new LECs in the framework of resonance saturation in terms of (dominant) $\Delta$ isobar and (small) vector meson excitations. The isobar contributions depend only on the strength of the $N\Delta$ transition magnetic moment. We have shown that for reasonable values of this constant, the 25% fourth-order loop corrections to the $P$-wave LETs are almost completely cancelled by the isobar terms. This solidifies the third-order LET predictions, which are in good agreement with the data, cf. eqs. (32),(33).

We are grateful to Reinhard Beck and Axel Schmidt for communicating the new MAMI data before publication.

## References

1. V. Bernard, N. Kaiser, U.-G. Meißner, Int. J. Mod. Phys. E **4**, 193 (1995).
2. U.-G. Meißner, in *Boris Ioffe Festschrift - "At the Frontier of Particle Physics–Handbook of QCD"*, Vol. **1**, edited by M. Shifman (World Scientific, Singapore, 2001) pp. 417–506, hep-ph/0007092.
3. R. Beck *et al.*, Phys. Rev. Lett. **65**, 1841 (1990).
4. M. Fuchs *et al.*, Phys. Lett. B **368**, 20 (1996).
5. A.M. Bernstein *et al.*, Phys. Rev. C **55**, 1509 (1997).
6. J.C. Bergstrom *et al.*, Phys. Rev. C **53**, (1996) R1052.
7. J.C. Bergstrom *et al.*, Phys. Rev. C **55**, 2016 (1997).
8. J.C. Bergstrom *et al.*, Phys. Rev. C **57**, 3203 (1998).
9. A. Schmidt *et al.*, submitted to Phys. Rev. Lett., nucl-ex/0105010.
10. V. Bernard, J. Gasser, N. Kaiser, U.-G. Meißner, Phys. Lett. B **268**, 291 (1991).
11. V. Bernard, N. Kaiser, U.-G. Meißner, Z. Phys. C **70**, 483 (1996).
12. V. Bernard, N. Kaiser, U.-G. Meißner, Phys. Lett. B **378**, 337 (1996).
13. S.R. Beane, V. Bernard, T.-S.H. Lee, U.-G. Meißner, U. van Kolck, Nucl. Phys. A **618**, 381 (1997).
14. J.C. Bergstrom, Phys. Rev. C **52**, 1986 (1995).
15. T.R. Hemmert, B.R. Holstein, J. Kambor, Phys. Lett. B **395**, 89 (1997); J. Phys. G **24**, 1831 (1998).
16. V. Bernard, T.R. Hemmert, U.-G. Meißner, in preparation.

17. N. Fettes, U.-G. Meißner, M. Mojžiš, S. Steininger, Ann. Phys. (N.Y.) **283**, 273 (2000).
18. P. Büttiker, U.-G. Meißner, Nucl. Phys. A **668**, 97 (2000).
19. N. Fettes, U.-G. Meißner, Nucl. Phys. A **679**, 629 (2001).
20. D.E. Groom *et al.* (Particle Data Group), Eur. Phys. J. C **15**, 1 (2000).